Structure and properties of hydrostatically extruded commercially pure titanium

S. Zherebtsov[a,*], W. Lojkowski[b], A. Mazur[b], G. Salishchev[a]

[a] Belgorod State University, Laboratory of Bulk Nanostructured Materials, 85 Pobeda Str, Belgorod, 308015, Russia
[b] Institute of High Pressure Physics, Polish Academy of Sciences, 29/37 Sokolowska Str, 01-142 Warsaw, Poland

A B S T R A C T

The effect of hydrostatic extrusion on the structure and mechanical properties of commercially pure titanium was investigated at 20 °C, 350 °C, and 450 °C, up to the true strain of e = 2. At 20 °C extrusion to e = 1.8 resulted in the formation of a lamellar-type microstructure with fragments of about 100 nm within the laths. Higher deformation temperatures lead to the formation of mixed microstructures consisting of packs of lamellae alternating with fine-grained areas. Hydrostatic extrusion results in a remarkable increase in the strength of titanium. The ultimate tensile strength of titanium extruded at 20 °C and 350 °C was 1080 and 765 MPa, respectively. The strength and elongation at the fracture can be controlled by varying the temperature of the extruded billet. The optimal deformation parameters for various applications are proposed.

Keywords:
Titanium
Hydrostatic extrusion
Grain refinement
Strength
Ductility

1. Introduction

The mechanical properties of metallic materials can be considerably improved by microstructure refinement [1]. In particular, the strength, fatigue resistance, and superplastic properties can be increased with decreasing grain size [1–4]. This goal of improving mechanical properties through grain refinement has contributed to the rapidly expanding field of materials engineering, in which ultrafine-grained materials are produced using severe plastic deformation (SPD). In pure metals, the grain size that can be obtained by SPD methods is typically in the range of 100-500 nm, and the resulting microstructure is called submicrocrystalline (SMC). However, in alloys it is possible to achieve grain sizes as small as 10 nm [cf. 5-10].

Well-established SPD techniques include high-pressure torsion [6], equal channel angular extrusion [7], and twist extrusion [8]. An advantage of these methods is the almost unlimited ability to accumulate deformation while maintaining the initial shape and size of the specimen. Repeated applications of standard deformation methods, such as rolling or compression, also result in the formation of SMC structures [9,10].

However, multi-pass deformation is costly and laborious; thus, technological processes which produce a high level of straining over one deformation cycle are very attractive. Hydrostatic extrusion (HE) is one such method, in which the billet is forced through a die by a liquid under high pressure. The use of high pressure lowers the brittle-to-ductile transformation temperature, and the pressure medium reduces friction during the extrusion process [11].

HE is suitable for working titanium [12,13], which has relatively low room temperature ductility due to its limited number of slip systems. Pachla et al. [12] showed that twenty passes of extrusion to the true strain of 5.47 can refine the microstructure to a grain size of 47 nm, and at that stage, the strength of the material increases to the remarkable value of 1320 MPa.

Heavy straining by means of HE can also be accomplished in one or two passes; this may be much more attractive than performing multiple passes. The magnitude of strain in one pass depends on the strength of the material and is limited by the capacity of the extruder. The degree of accumulative strain increases with the billet temperature. However, the effect of increased temperature on the structure and properties of titanium during HE is not yet well understood. In the present work, the evolution of the microstructure and the mechanical properties of commercially pure titanium under HE was studied, using an initial billet temperature in the range 20 °C to 450 °C.

2. Experimental procedures

Commercially pure titanium VT1-0 was used in this study. The titanium had a nominal chemical composition (in wt.%), of Ti - 0,18 Fe - 0,1 Si–0,07 C - 0,04 N - 0,12 O, and it was supplied as a hot-rolled bar ⌀25 mm. Specimens measuring 22 mm diameter × 50 mm length were machined from the bar. In its initial condition, the titanium has a homogeneous microstructure with a mean grain size of 30 μm.

* Corresponding author. Tel.: +7 4722 585416; fax: +7 4722 585415.
E-mail addresses: Zherebtsov@bsu.edu.ru, ser_z@mail.ru (S. Zherebtsov).

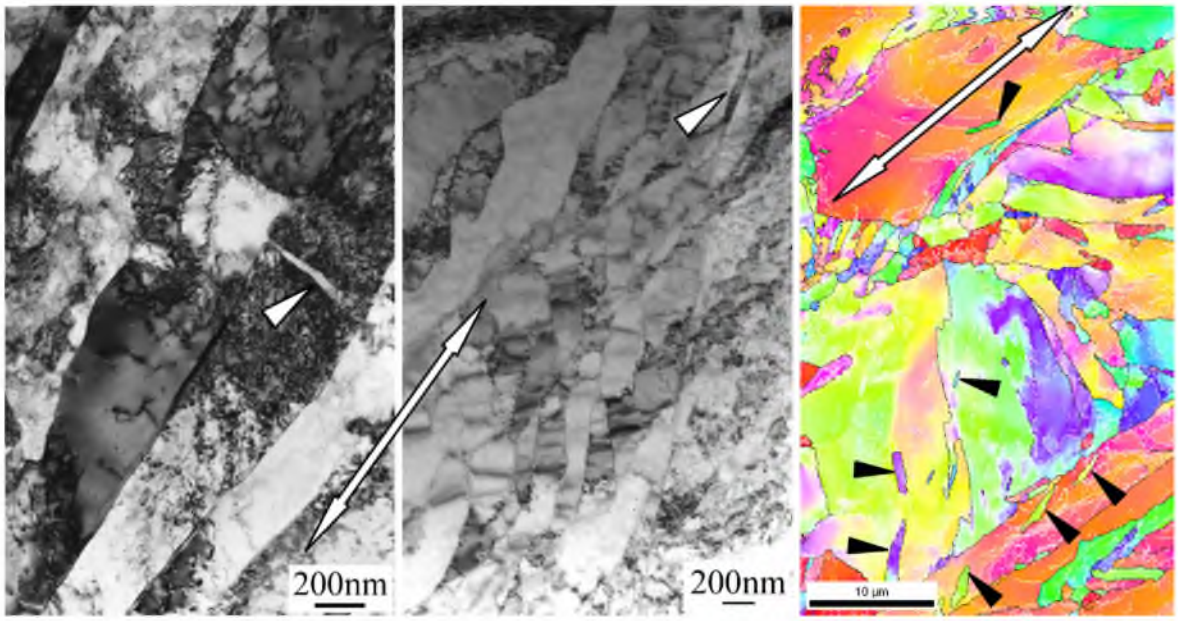

Fig. 1. Microstructure of titanium after HE at 20 °C to e = 0.7; (a and b) – TEM images, (c) – EBSD map. Extrusion direction is indicated by arrows. Also some twins are indicated by triangle marks.

Hydrostatic extrusion was conducted at temperatures below 450°C. Severe deformation at these temperatures ensures the formation of a SMC structure in titanium [14]. To avoid chilling during extrusion and to increase the macroscopic homogeneity of the deformation, the specimens subjected to HE at elevated temperatures were inserted into cupper containers 50 mm in diameter and 250 mm in length. The containers with the specimens were heated in an air furnace at 350 °C or 450 °C, and then inserted into the high pressure vessel of the hydrostatic extruder. The delay before the extrusion was 15-20 sec. At room temperature (20 °C) no containers were used for the HE and one or two passes were used for the extrusion.

The deformation was carried out in a horizontal hydrostatic extruder operating at pressures of up to 1.5 GPa. Castor oil was the working fluid. The strain rate during hydrostatic extrusion was approximately 40 mm/sec ($\sim 10^{-1} s^{-1}$). A cone die with an angle of 30° at room temperature and of 90° at higher temperatures was used for the extrusion.

The extruded samples were air cooled. The titanium core was extracted from the container using turning. The true strain of the extruded samples was calculated as $e = \ln(F_0/F)$, where F_0 and F are the initial and final cross-sectional areas, respectively. Four samples were produced: two samples formed at 20°C with strains of 0.7 and 1.8 (after the second pass), one sample at 350°C with a strain of 1.8, and the final sample at 450°C with a strain of 2.

The microstructure of the extruded samples was investigated along the longitudinal section, using a JEM-2000 EX transmission electron microscope (TEM) at the accelerating voltage 200 kV, a LEO-1530 scanning electron microscope (SEM), and optical microscopy.

A high resolution electron back scattering diffraction (EBSD) analysis was conducted using a Quanta 600 FEG SEM equipped with TSL OIM™ software. Orientation mapping was performed with automated beam control using a triangular scanning grid; the corresponding step size was 0.1 μm. The grain-dilation function in the TSL software was used to automatically remove small grains from the maps if they comprised three or fewer pixels. Boundaries having a misorientation less than 2° were eliminated from consideration, since the experimental accuracy of the EBSD method for orientation evaluation typically does not exceed one degree [15]. A misorientation of 15° was selected as the upper limit for the low-angle boundaries. Since the grain shapes where highly irregular, the grain area was estimated instead of the grain diameter.

The rate of misorientation change was measured using the TSL software, and is defined as the average change of misorientation per unit length during a linear scan of the sample. This rate provides a measure of the density of grain boundaries and their average misorientation.

The tensile tests were carried out at room temperature using cylindrical samples having a gage size of 3 mm in diameter and 18 mm in length.

3. Results

3.1. Microstructure of titanium after hydrostatic extrusion at 20 °C

A TEM examination of the sample that was extruded at 20 °C to e = 0.72 revealed a heterogeneous microstructure consisting of lamellae mainly aligned along the extrusion axis (Fig. 1a,b). The widths of the lamellae vary from a hundred nanometers to a few micrometers. The boundaries of the lamellae are straight and thin (Fig. 1a); some of these boundaries display extinction contours that may imply medium or high misorientation. In some places the dislocation walls or low-angle sub-boundaries form a sub-grain structure (Fig. 1b). The widths of the sub-grains are about 200 nm, and the length usually exceeds 1 μm. The dislocation density in the microstructure is relatively high; however, there are lamellae containing only isolated dislocations.

A misorientation map obtained by an EBSD analysis is shown in Fig. 1c. The microstructure consists of a few lamellae that are separated by high-angle boundaries and aligned along the extrusion axis (right bottom corner of Fig. 1c). However, there are a number of high-angle boundaries which are almost perpendicular to the extrusion axis (central part of Fig. 1c). The space between these latter boundaries may reach 10 μm. Large grains having areas of 100-200 μm^2 are observed in the microstructure; also observed

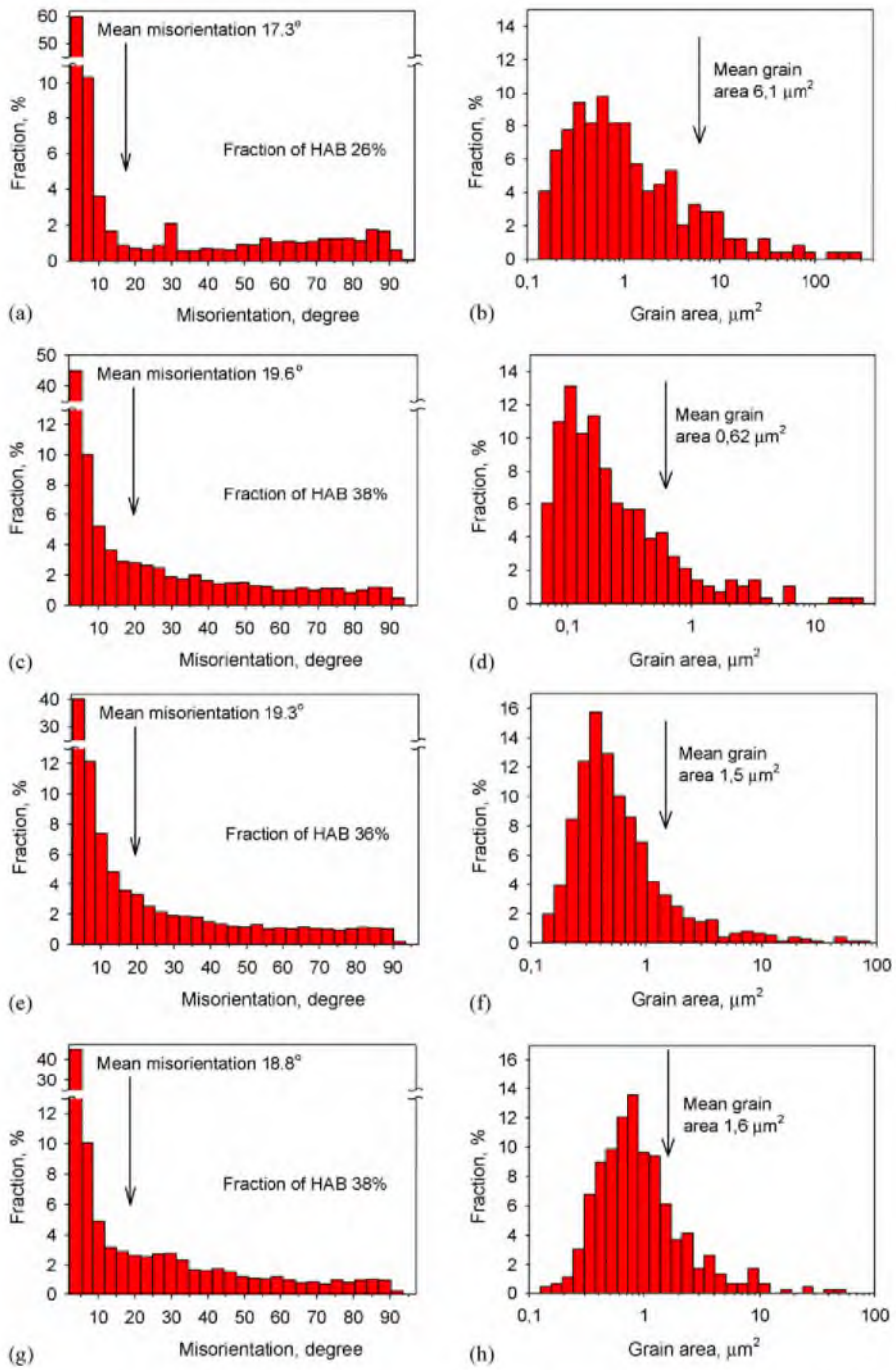

Fig. 2. Misorientation distribution (a, c, e, g) and grain area distribution (b, d, f, h) of titanium hydrostatically extruded at (a, b) T = 20 °C, e = 0.7; (c, d) T = 20 °C, e = 1.8; (e, f) T = 350 °C, e = 2.0; (g, h) T = 450 °C, e = 1.8.

are a large fraction of small grains having areas ~0.1 μm^2 (Fig. 2b). The mean grain area was 6.1 μm^2. The distribution of the boundary misorientation angles shows a pronounced low-angle peak that is typical of a cold-worked condition. However, there is a considerable fraction of high-angle boundaries, as indicated by the mean misorientation of 17° which corresponds to a lower misorientation range of high-angle grain boundaries (Fig. 2a). Three local peaks are clearly seen in the misorientation spectra, at approximately 28°, 57°, and 87° (marked in Fig. 2a by arrows). Some of them can be associated with twin boundaries, such as the {101} twin with a misorientation of 57°, and {102} and {113} with misorientations of 84.78° and 86.98°, respectively. Some of these twins are indicated by triangle marks in Fig. 1.

The further extrusion of titanium at 20°C to a total strain e = 1.8 results in the formation of a lamellar microstructure, with lamellae widths in the range of 100-500 nm. All the lamellae are aligned with the extrusion axis. In some areas the dislocation density is extremely high, so that boundaries between the lamellae are barely seen (Fig. 3a). In those cases the lamellae are short with curved boundaries. Conversely, in areas that have a relatively low dislocation density, the lamellae are long and straight with clear boundaries (Fig. 3b).

On the EBSD map, the structure shows a lamellar morphology with lamellae of varying widths and lengths (Fig. 3c). The mean grain area is about 0.6 μm^2, and the grain area distribution is narrower than for e = 0.7. Nevertheless, there is a fraction of relatively

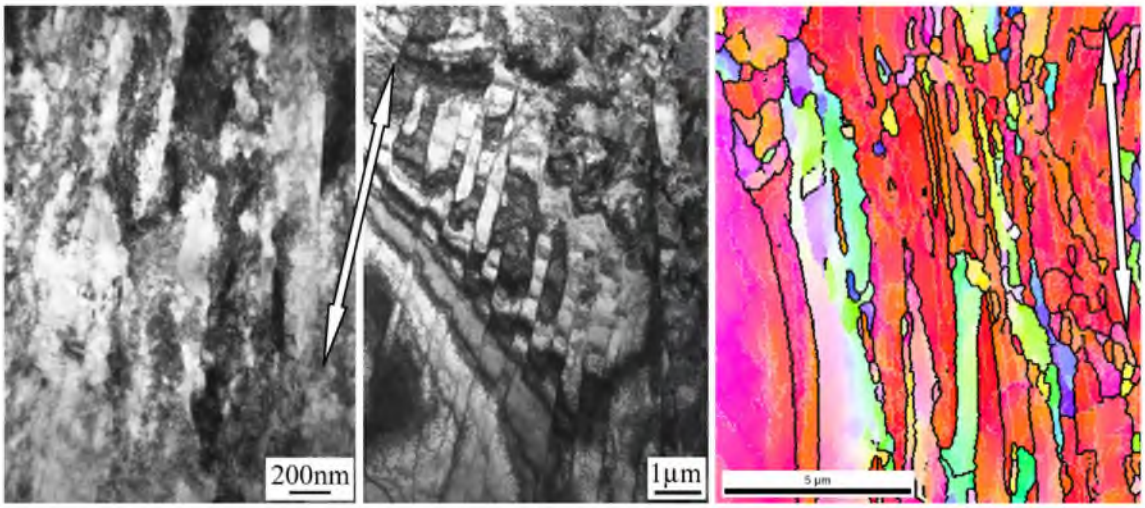

Fig. 3. Microstructure of titanium after HE at 20 °C to e = 1.8 in two passes; (a and b) – TEM images, (c) – EBSD map. Extrusion direction is indicated by arrows.

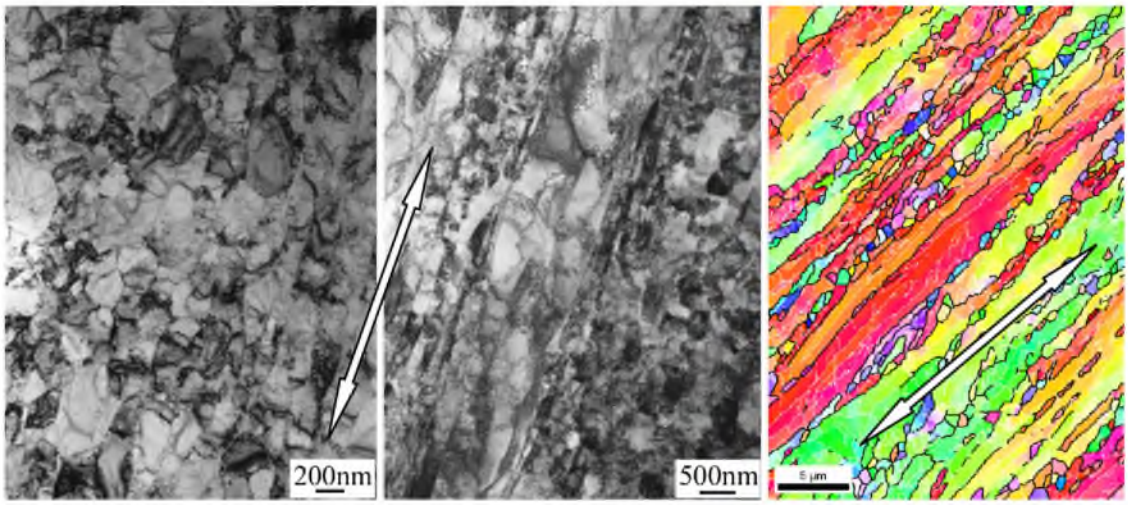

Fig. 4. Microstructure of titanium after HE at 350 °C to e = 2.0; (a and b) – TEM images, (c) – EBSD map. Extrusion direction is indicated by arrows.

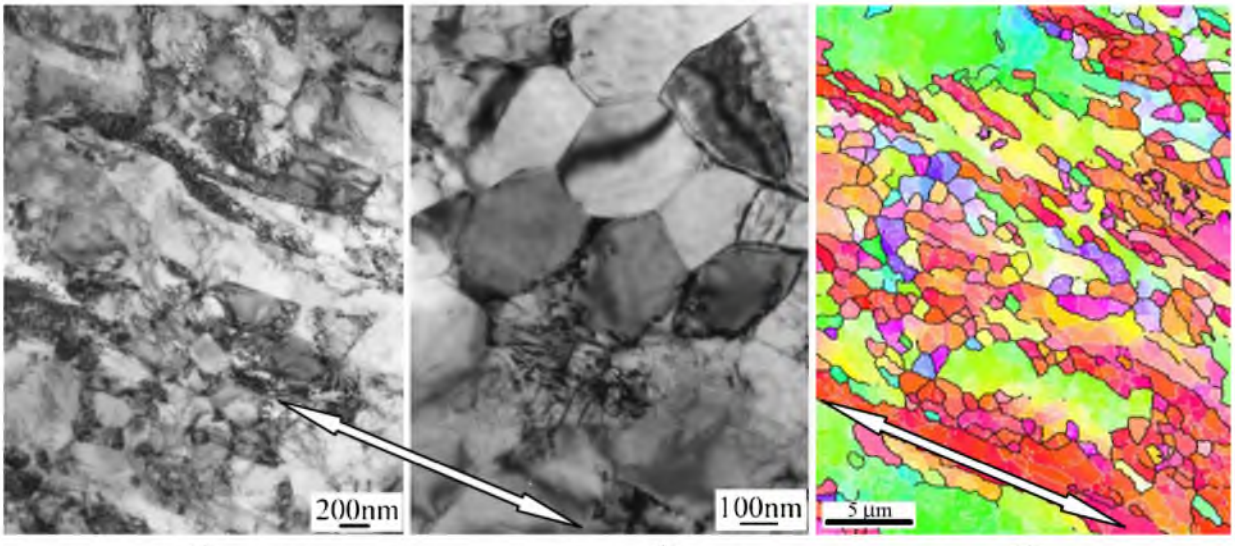

Fig. 5. Microstructure of titanium after HE at 450 °C to e=1.8; (a and b) – TEM images, (c) – EBSD map. Extrusion direction is indicated by arrows.

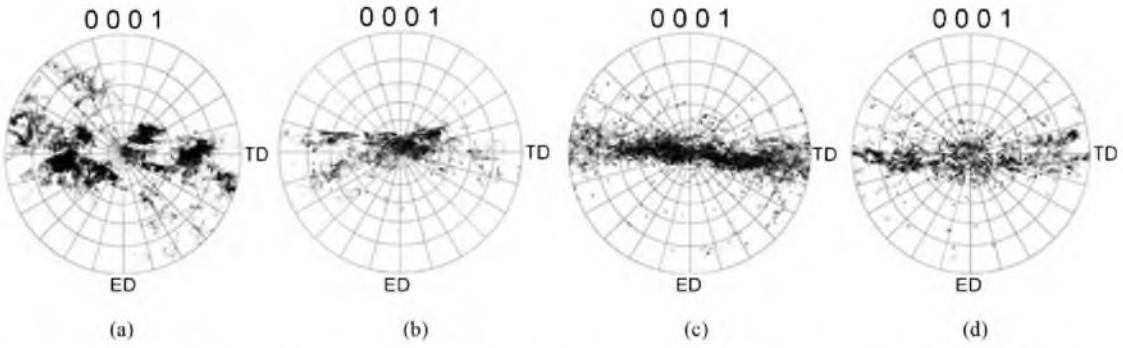

Fig. 6. Pole figures (0001) obtained from hydrostatically extruded titanium: (a) T=20 °C, e=0.7; (b) T=20 °C, e=1.8; (c) T=350 °C, e=2.0; (d) T=450 °C, e=1.8.

large grains (up to 20 μm^2) in the structure. The fraction of high-angle boundaries increases to 38% (compared with 26% for e = 0.7, Fig. 2). There are very small peaks in the misorientation distribution at 65°, 75°, and 87°, which may imply a small fraction of twin boundaries in the structure after this higher strain.

3.2. *Microstructure of titanium after hydrostatic extrusion at 350 °C and 450 °C*

Deformation at the higher temperature of 350 °C results in the formation of a mixed lamellar/granular microstructure, in which long lamellae alternate with bands of small globular grains (Fig. 4). The lamellae width reaches 5 μm, and the lamellae have longitudinal boundaries (mainly low-angle, judging by the EBSD map) separated by about 0.5 μm (Fig. 4b). With a background of relatively high dislocation density, there are grains which are almost free of dislocation (Fig. 4a). The presence of long and wide lamellae widens the grain area distribution; however, due to a large fraction of grains of 0.2-0.3 μm^2, the mean grain area is 1.5 μm^2 (Fig. 2f). The mean misorientation (19.3°) and the fraction of high-angle boundaries (36%) are nearly the same as those observed in the microstructure after HE at 20 °C to e = 1.8 (Fig. 2c,e).

Hydrostatic extrusion at 450 °C changes the character of the microstructure (Fig. 5). The lamellae become much shorter and somewhat wider (Fig. 5a, c) compared with those resulting from deformation at 350°C. The fraction of large grains does not decrease considerably compared to the case at 350 °C (Fig. 2h). However, the area of new small grains increases to about 0.7 μm^2, so that the mean grain area increases slightly to 1.6 μm^2. Groups of globular dislocation-free grains occur (Fig. 5b). Triple junctions with an angle close to 120°, and straight boundaries between the grains, imply the occurrence of a recrystallization process. The fraction of high-angle boundaries and the mean misorientation are similar to those observed after extrusion at 350 °C (Fig. 2g). It is interesting to note the appearance of a pronounced peak at 30° in the misorientation distribution. The only other observation of a similar peak was in a specimen extruded at 20 °C to e = 0.7.

3.3. *Texture of titanium after hydrostatic extrusion at 20 °C, 350 °C, and 450 °C*

Pole figures (0001) were obtained by an EBSD analysis of titanium extruded at 20 °C, 350 °C, and 450 °C; these are shown in Fig. 6. In all cases the texture is axial, with the *c*-axis of the HCP lattice oriented along the radius of the extruded bar [16]. After extrusion at 20 °C to e = 0.7, the pattern consists of a few clusters originating from large areas having similar orientations (Figs. 1c, 6a). Further extrusion at the same temperature to e = 1.8 leads to the formation of a texture in which the basal plane of the HCP lattice is mainly parallel to the specimen surface (Figs. 3c, 6b). With extrusion at 350 °C (Fig. 4c), a sharp axial texture is observed in the specimen (Fig. 6c). Increasing the extrusion temperature to 450 °C (Fig. 5c) causes the texture to become more scattered (Fig. 6d).

EBSD analyses were performed for each condition as the point-to-origin misorientation changes with distance. The rate of this change as a function of temperature is shown in Fig. 7. It is clearly seen that the misorientation changes much faster in the specimen extruded at 20 °C to e = 1.8, compared with the specimens extruded at 350 °C and 450 °C. However, there is almost no effect on the rate of misorientation change as the temperature increases from 350 °C to 450 °C.

3.4. *Mechanical properties of titanium after hydrostatic extrusion at 20 °C, 350 °C, and 450 °C.*

Engineering stress-strain curves for the specimens obtained during the tensile test are shown in Fig. 8. Titanium extruded at 20 °C to e = 1.8 is the strongest (Table 1). Hydrostatic extrusion at 20 °C to e = 0.7 and at 350 °C to e = 2.0 results in rather similar strength of the titanium, at a value about 30% lower than the maximum strength. Extrusion at 450 °C to e = 1.8 increases the strength of the titanium by 30% compared to the initial condition (Table 1). The ductility of the specimens in terms of tensile elongation decreases as the strength increases, with the exception of the specimen obtained by extrusion at 20 °C to e = 0.7. This specimen has medium strength and the minimum tensile elongation.

Compared to the initial condition, HE decreases tensile elongation by a factor of 1.5 - 2. It interesting to note the shape of the stress-strain curve in terms of its deformation before necking. After extrusion at room temperature, the deformation before necking increases from 0.75% to 2% as the strain increases from 0.7 to 1.8. An increase in the extrusion temperature to 350 °C and 450 °C

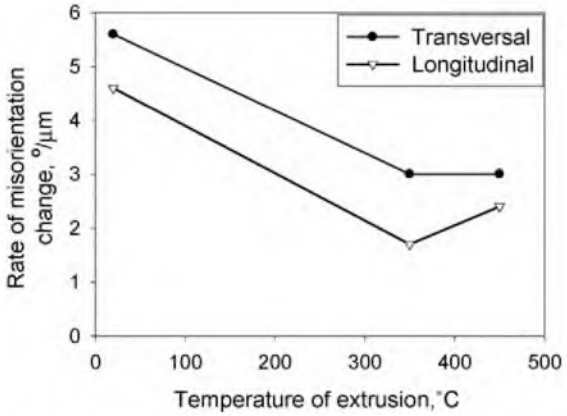

Fig. 7. Rate of the misorientation change as a function of HE temperature.

Table 1
Mechanical properties of the hydrostatically extruded titanium.

Condition	YS, MPa	UTS, MPa	AR, %	TE, %	A, kJ/m^3
Initial	360	490	73	29	129
SMC [14]	760	810	63	18	-
Extrusion at 350 °C to e = 2	624	765	42	16	110
Extrusion at 450 °C to e = 1.8	557	642	48	21	122
Extrusion at 20 °C to e = 0.7	700	715	48	12	-
Extrusion at 20 °C to e = 1.8	985	1080	32	14	125
Extrusion at 20 °C to e = 5.47 [12]	1245	1320		7,5	84

YS: yield stress; UTS: ultimate tensile strength; AR: area reduction; TE: total elongation; A: work of deformation to failure.

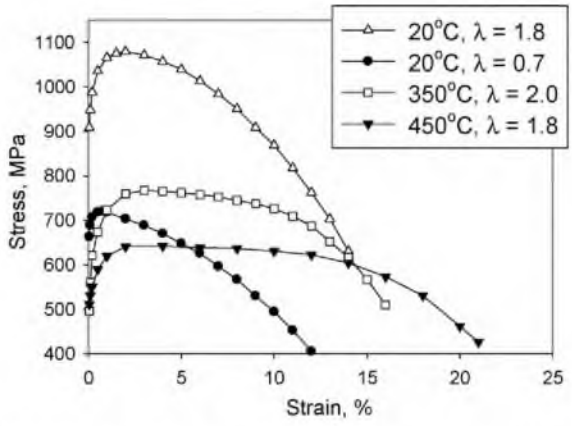

Fig. 8. Engineering stress-strain curves for the hydrostatically extruded titanium.

increases the deformation before necking to 3% and 4%, respectively (Fig. 8).

4. Discussion

Formation of a lamellar-type microstructure after heavy cold working is well documented for various materials having FCC and BCC lattices [16–21]. The transformation of a globular microstructure into a lamellar one during large deformation is associated with the creation of deformation-induced boundaries (DIBs) [17,19]. DIBs create a specific lamellar microstructure, in which boundaries between lamellae (geometrically necessary boundaries - GNBs) separate regions that are deformed by different slip system combinations. GNBs differ from incidental dislocation boundaries (IDBs), which are ordinary cell boundaries that form by the trapping of glide dislocations. The formation of GNBs with moderate-to-high misorientation occurs after a relatively high strain level [17].

Pure titanium has only four independent slip modes at ambient temperature, which involve basal, prismatic, and pyramidal slip. These all have a Burgers vector in the basal plane; therefore, the tension or compression along the ***c*** axis is accommodated by twinning. As one of the main deformation modes, twinning in titanium occurs in the earliest stages of deformation. Therefore, in the present work, a large fraction of high angle boundaries (HABs) after a relatively small strain (e = 0.7) is obviously due to twinning (Fig. 2a). Only when the dislocation density becomes high enough to suppress twinning [22] does the microstructure evolve by the formation of DIBs (Fig. 1).

Some of the peaks in the high-angle area after e = 0.7 are associated with {101}, {102}, and {113} twins. Among them, {102} <101> is supposedly a primary twinning system at a high level of strain [23], while the others are secondary twins. It is interesting to note that a peak at 30° is associated with a Σ13a coincident-site-lattice (CSL) boundary, rather than with a twin boundary. Other authors [23,24] have also observed the peak at 30° in the structure of cold-worked titanium, but no unified explanation of its formation has been proposed. In [24], this phenomenon was ascribed to a predominant prismatic sliding. However, at 450°C CSLs may also result from the dissociation of boundaries during a recrystallization process [16]. With further deformation, twin CSL boundaries transform into random HABs, due to the trapping of lattice dislocations.

An increase in strain to e = 1.8 increases microstructure homogeneity and considerably decreases the grain size compared with e = 0.7. There is a large fraction of small grains with a grain area of 0.1-0.2 μm^2 (Fig. 2d); however, relatively large lamellar areas are also observed which comprise only low-angle boundaries (Fig. 3). The misorientation distribution and sharpness of the specimen's pole figure is typical for a heavily cold worked material (Figs. 2c and 6b), but the presence of large areas without high-angle boundaries indicates that the strain level was still insufficient to achieve a uniform ultrafine-grained microstructure. Nevertheless, this material has very good mechanical properties despite some microstructure inhomogeneities, making it similar to a medium-strength titanium alloy (for example, Ti-6Al-4 V).

The relationship between the yield stress σ_y and grain size D was proposed by E.O. Hall and N.J. Petch in the form $\sigma_y = \sigma_o + kD^{-1/2}$,

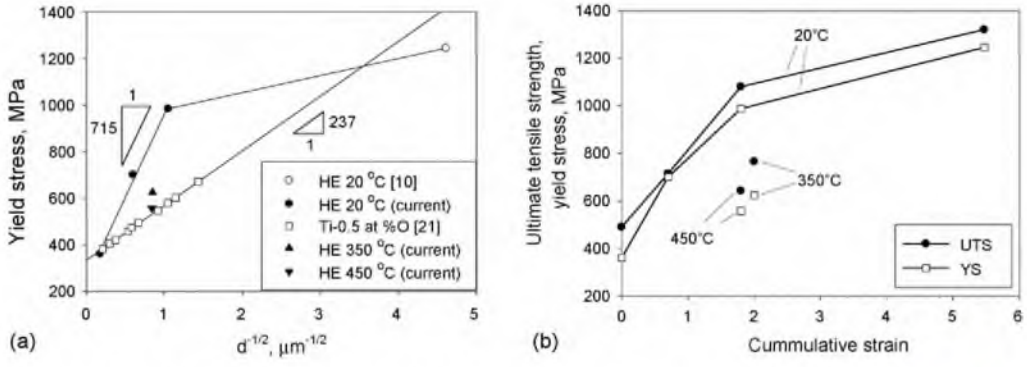

Fig. 9. Strength of titanium as a function of (a) grain size (Hall–Petch relationship); (b) cumulative strain of HE (cf. Table 1).

where σ_0 is the frictional stress required to move dislocations within grains, and k is a constant associated with the transfer deformation across grain boundaries. Data from the present study (filled circles in Fig. 9a) follow the Hall–Petch relationship reasonably well; however, the slope is larger by a factor of 3 compared with the slope reported by Conrad [25] for a titanium sheet with 0.5 at.% oxygen (open squares in Fig. 9a).

It is obvious that the strength of heavily deformed materials is not solely a result of grain size strengthening, but is a superposition of multiple strengthening factors. The effect of those factors inevitably leads to a deviation from the conventional Hall–Petch relationship [17,18,26–28]. The influence of various strengthening mechanisms on the Hall–Petch relationship have been considered in a number of papers: modifications to the Hall–Petch relation have included the effect of substructural strengthening and high dislocation density [17,26], the non-equilibrium state of grain boundaries [27], the residual stress [18], and the shape anisotropy of the grains [28]. In the present case, the deviation from the Hall–Petch relationship is cumulative due to various strengthening factors; their total value is 49% and 70% (for strain e = 0.7 and 1.8, respectively) of the conventional Hall–Petch relation obtained by Conrad [25]; these values are in reasonable agreement with the data reported in [18,27] (50 and 54%, respectively). The deformation nature of the strengthening factors is supported by the observation that after hydroextrusion at elevated temperatures (when the influence of residual stress, sub-structural strengthening and a non-equilibrium state of grain boundaries is relatively low) the strength of samples almost falls back to the Hall–Petch line for titanium (Fig. 9a).

It is important to note the data obtained by Pachla et al. for commercial purity titanium [12] that was subjected to twenty passes of hydrostatic extrusion to the true strain of 5.47 (open circle in Fig. 9a). This result is rather close to Conrad's plots [25], but does not fit with the present results. It is known [29] that the slope of the Hall–Petch relationship decreases in the area of nanograins, which implies that Pachla's data is in good agreement with the Hall–Petch relation for titanium having extremely small grains.

However, in this case the strength of the material at very high strain is almost completely compensated by grain size strengthening only, while the influence of deformation-induced factors of strengthening vanishes. Indeed, it was shown that the size of grains and subgrains become equal [30,31], and the internal stresses attain a saturation level [4,32] after large deformation. Consequently, during the first steps of HE all of these factors contribute to the increased slope of the strength - grain size curves (Fig. 9a). However, the effect of sub-structural strengthening and residual stresses decreases with strain, and in case of room temperature HE, saturates in the interval e = 2÷3. Importantly, a similar result is obtained by comparing the present data with the results obtained by Pachla et al. for titanium subjected to twenty passes of hydrostatic extrusion to the true strain of 5.47 [12]: HE rapidly increases the strength of the material until e = 2÷3 (Fig. 9b), at which point the strength increase slows down.

In contrast to other severely deformed materials, titanium after HE has rather attractive ductile characteristics. Although the uniform elongation of the specimen after HE at room temperature to e = 1.8 is only 2%, the ability of the extruded material to strain harden is much higher than it is with titanium worked by other SPD methods. For example, the difference between the ultimate tensile strength and the yield stress in our case and in [12] is almost 100 MPa, while for other SPD methods the difference is only about 30-50 MPa [14,33,34].

An explanation for this effect may be, that HE is accompanied by adiabatic heating of the material in the die area up to 150 °C [35]; however, the temperature drops abruptly as soon as the extruded part of the bar exits from the die. This short thermal effect may explain the formation of small grains with relatively low dislocation density (Figs. 4 and 5), the reduction of internal stains, the equilibration of the grain boundary structure, and the considerable changes to the shape of the stress-strain curves (Fig. 8).

HE at elevated temperature leads to dynamic recrystallization, which occurs during or just after extrusion. Recrystallization results in the formation of new globular grains along the deformation-induced boundaries. The diameter of the grains is in the range 0.4-0.5 μm. Interestingly, a sharper texture in the case of warm extrusion is associated with a noticeably lower intensity of misorientation increase with distance (Fig. 7). Such structural changes decrease the strength and increase the deformation before necking and tensile elongation. Similar results have been observed after short-term aging of heavily deformed specimens [4].

The area under the engineering curves can be regarded as a measure of the work of deformation to failure (A, kJ/m^3) of the material, and an indirect measure of its toughness. The curves corresponding to 20 °C, 350 °C, 450 °C, with e = 1.8-2, provide similar results (Table 1), with work of deformation slightly lower than that of the initial condition.

Among all conditions considered in the present study, the material extruded at 350°C is the most promising from a practical point of view. Due to the very high deformation rate under hydrostatic pressure and the adiabatic heating effects, the fine-grained structure of this condition comprises areas with relatively low dislocation density, and narrow, almost dislocation-free, high-angle GNBs (Fig. 3b). According to [36], the presence of relatively large recrystallized grains in a very fine-grained microstructure may improve the stability of plastic flow and increase ductility.

Consequently, by varying the billet temperature it is possible to optimally balance strength and ductility for a given application, without loss in fracture toughness. Evaluation of the work of deformation to failure implies that, in contrast to other high-strength states of titanium obtained by various SPD methods [14,33,34], HE does result in high levels of strength, ductility, and toughness. Multiple extrusions to e = 5.47 considerably decreases the work of deformation; thus, heavily strained materials have only limited applicability to the production of critical parts, despite having very high strength. Also, due to obvious technological limitation, large deformation (e > 2) during HE may be attained only by two or more passes of extrusion, which increases the laboriousness of the process considerably. Based on the obtained results, HE accomplished in one or two passes is promising for producing bars of titanium with very high strength and reasonable ductility.

5. Conclusions

We investigated the effect of hydrostatic extrusion on the structure and mechanical properties of commercial pure titanium, extruded at 20 °C, 350 °C, and 450 °C, up to the true strain of e = 2. Extrusion at 20 °C to e = 1.8 resulted in the formation of a lamellar-type microstructure, with the width of the lamellae in the range 100-500 nm. At the higher deformation temperatures of 350 °C and 450 °C, mixed microstructures formed consisting of packs of lamellae alternating with fine-grained areas. Hydrostatic extrusion leads to a remarkable increase in titanium strength; the ultimate tensile strength of titanium extruded at 20 °C was found to be 1080 MPa. Extrusion at a higher temperature decreases the strength but also increases the ductility of the material, so that the work of deformation to failure remains almost unchanged.

The use of the appropriate temperature for HE allows an optimum balance between strength and ductility without loss in fracture toughness. The best strength/ductility combination depends upon the planned application of the material.

Acknowledgements

This work was supported by Federal Agency for Education, Russia, under Grant No. P2486.

References

[1] R.W. Armstrong, Metall. Trans A1 (1970) 1169–1176.
[2] M.A. Meyers, A. Mishra, D.J. Benson, Prog. Mater. Sci. 51 (2006) 427–556.
[3] K.S. Kumar, H. Van Swygenhoven, S. Suresh, Acta Mater 51 (2003) 5743–5774.
[4] R.Z. Valiev, R.K. Islamgaliev, I.V. Alexandrov, Prog. Mater. Sci 45 (2000) 102–189.
[5] Yu. Ivanisenko, W. Lojkowski, R.Z. Valiev, H.J. Fecht, Acta Mater 51 (2003) 5555–5570.
[6] R.Z. Valiev, T.G. Langdon, Prog. Mater. Sci 51 (2006) 881–981.
[7] A.P. Zhilyaev, T.G. Langdon, Prog. Mater. Sci 53 (2008) 893–979.
[8] Y. Beygelzimer, V. Varyukhin, S. Synkov, D. Orlov, Mater. Sci. Eng A503 (2009) 14–17.
[9] N. Tsuji, Y. Saito, H. Utsunomiya, S. Tanigawa, Scripta Mater 40 (1999) 795–800.
[10] S.V. Zherebtsov, G.A. Salishchev, R.M. Galeyev, O.R. Valiakhmetov, S.Yu. Mironov, S.L. Semiatin, Scripta Mater 51 (2004) 1147–1151.
[11] J.J. Lewandowski, P. Lowhaphandu, Int. Mater. Rev 43 (1998) 145–187.
[12] W. Pachla, M. Kulczyk, M. Sus-Ryszkowska, A. Mazur, K.J. Kurzydlowski, J. Mater. Process. Tech 205 (2008) 173–182.
[13] H. Garbacz, M. Lewandowska, W. Pachla, K.J. Kurzydłowski, J. Microscopy 223 (2006) 272–274.
[14] G.A. Salishchev, R.M. Galeev, S.P. Malysheva, S.V. Zherebtsov, S.Yu. Mironov, O.R. Valiakhmetov, E.I. Ivanisenko, Met. Sci. Heat. Treat 48 (2006) 63–68.
[15] F.J. Hamphreys, J. Microscopy 195 (1999) 170–185.
[16] F. Humphreys, M. Hatherly, Recrystallization and Related Annealing Phenomena, second ed., Elsevier, Oxford, 2004.
[17] D.A. Hughes, N. Hansen, Acta Mater 48 (2000) 2985–3004.
[18] A. Belyakov, K. Tsuzaki, Y. Kimura, Y. Mishima, Philos. Mag. Lett 89 (2009) 201–212.
[19] V.V. Rybin, Severe Plastic Deformations and Fracture of Metals, Metallurgiya, Moscow, 1986.[in Russian].
[20] N. Hansen, D.J. Jensen, Phil. Trans. R. Soc. Lond A357 (1999) 1447–1469.
[21] G.I. Rosen, D.J. Jensen, D.A. Hughes, N. Hansen, Acta Met. Mater 43 (1995) 2563–2579.
[22] J.W. Christian, S. Mahajan, Prog. Mater. Sci 39 (1995) 1–157.
[23] Y.B. Chun, S.H. Yu, S.L. Semiatin, S.K. Hwang, Mater. Sci. Eng A398 (2005) 209–219.
[24] S.Yu. Mironov, M.M. Myshlyaev, Phys. Solid. State 49 (2007) 858–864.
[25] H. Conrad, Prog. Mater. Sci 26 (1981) 123–403.
[26] M.A. Meyers, K.K. Chawa, Mechanical Behavior of Materials, Cambridge University Press, New York, 2009.
[27] N. Krasilnikov, W. Lojkowski, Z. Pakiela, R. Valiev, Mater. Sci. Eng A397 (2005) 330–337.
[28] K.J. Kurzydłowski, B. Ralph, Quantitive description of microstructure of materials, CRC Press, Baton Rouge, 1995.
[29] M.A. Meyers, A. Mishra, D.J. Benson, Prog. Mater. Sci 51 (2006) 427–556.
[30] A. Belyakov, T. Sakai, H. Miura, K. Tsuzaki, Philos. Mag A81 (2001) 2629–2643.
[31] A. Belyakov, K. Tsuzaki, H. Miura, T. Sakai, Acta Mater 51 (2003) 847–861.
[32] S.V. Zherebtsov, R.M. Galeev, G.A. Salishchev, M.M. Myshlyaev, Phys. Met. Metallogr 87 (1999) 318–323.
[33] V. Latysh, G. Krallics, I. Alexandrov, A. Fodor, Current Appl. Phys 6 (2006) 262–266.
[34] A.Y. Vinogradov, V.V. Stolyarov, S. Hashimoto, R.Z. Valiev, Mater. Sci. Eng. A318.
[35] M. Kulczyk, W. Pachla, A. Mazur, R. Diduszko, H. Garbacz, M. Lewandowska, W. Łojkowski, K.J. Kurzydłowski, Mater. Sci. Poland 23 (2005) 839–846.
[36] Y.M. Wang, E. Ma, Acta Mater 52 (2004) 1699–1709.